ORIGINAL RESEARCH ARTICLE

Nicotine Population Pharmacokinetics in Healthy Smokers After Intravenous, Oral, Buccal and Transdermal Administration

Per O. Olsson Gisleskog[1,6] · Juan José Perez Ruixo[2] · Åke Westin[3] · Anna C. Hansson[4] · Paul A. Soons[5]

Abstract

Background In 4 decades, numerous nicotine replacement therapy products have been developed. Population pharmacokinetic models can support exposure–response modeling and inform nicotine replacement therapy product development, but only limited model-based cross-study population pharmacokinetic analyses for nicotine replacement therapy products have been published.

Objectives The aim of this retrospective analysis was to assess the population pharmacokinetics of nicotine across intravenous, oral, transdermal and oromucosal (mouth spray, chewing gum, lozenge and inhaler) routes and formulations in healthy smoking subjects.

Methods Data on 930 unique subjects (46,016 observations) from 29 single- and repeated-dose studies with multiple formulations across intravenous, oral, transdermal and oromucosal routes of administration were included. Data from intravenous and extravascular routes of administration were modelled separately for run efficiency reasons. For developing extravascular models, clearance and disposition parameters and their inter-individual variabilities were fixed to the estimates for intravenously delivered nicotine. Detectable pre-dose nicotine concentrations were modelled as a hypothetical nicotine bolus into the central compartment at the start of wash-out. Modelling repeated-dose oral and buccal administrations required a time-dependent increase in clearance or decrease in bioavailability to describe the data adequately.

Results Disposition of intravenous nicotine was best described by a three-compartment model with initial and terminal half-lives of 7 min and 4.5 h, respectively, and the absorption of single oral doses was best described with a first-order absorption rate constant of 1.55 h^{-1}. The data of buccal formulations were modelled with parallel oromucosal absorption and gastrointestinal absorption of a part of the dose that is swallowed. For transdermal nicotine, parallel zero- and first-order release from the patch and a transit-compartment absorption model best described the data. Key pharmacokinetic parameters were reliably estimated, with typical values for clearance (67 L/h for a 70-kg subject), volume of distribution (4.3 L/kg), oral bioavailability (40%) and transdermal bioavailability (76%) within expected ranges. The estimated fraction of the dose swallowed for buccal formulations ranged from 55% (gum) to 69% (lozenge).

Conclusions Robust population pharmacokinetic models were developed for five nicotine replacement therapy product types and for intravenous and oral nicotine. These population pharmacokinetic models are used in exposure–response analyses and simulation-based nicotine replacement therapy product design.

✉ Paul A. Soons
psoons@its.jnj.com

Extended author information available on the last page of the article

1 Introduction

Tobacco use is a major public health concern. Cigarette smoking is the leading cause of preventable death, estimated at over 7 million avoidable deaths per year worldwide and trending upwards [1–3]. Many of these deaths are directly or indirectly caused by lung cancer, chronic obstructive pulmonary disease, or cardiovascular diseases, and the total health burden of tobacco use is even larger. Although nicotine is the substance in tobacco responsible for smoking addiction, mostly other constituents of combusted tobacco are linked

Key Points

A large nicotine blood-concentration dataset for seven different nicotine products was retrospectively reanalysed

Population pharmacokinetic models were developed, and model parameters were estimated precisely

These models are available to help the development of new nicotine replacement therapy products

to health problems [4]. Nicotine replacement therapy (NRT) substitutes nicotine from tobacco products through other means of administration. Most clinically used NRT treatments are designed for oromucosal (i.e. buccal and sublingual) absorption. Nicorette gum, the first NRT product, was first registered in Switzerland in 1978. Since then, a number of different dosage forms for oromucosal absorption have been introduced, among them mouth spray, lozenges, sublingual tablets and inhalers. Nicotine replacement therapy has been shown to increase the relative smoking abstinence rate compared with placebo with 50–70% [5] and is an important tool in achieving reduction in tobacco use and lung cancer incidence [6].

Knowledge of nicotine pharmacokinetics is central to understanding its role in addiction. After intravenous (iv) administration, nicotine is extensively distributed to body tissues, including the brain, with a steady-state volume of distribution averaging 136–213 L (1.8–3.3 L/kg), exceeding corporal water volume [7–12]. After inhalation (e.g. smoking), nicotine is very rapidly distributed to the brain. In contrast to inhalation from smoking, the transdermal, gastrointestinal, oromucosal and nasal routes of absorption result in a more gradual increase of nicotine concentrations in the brain and other peripheral tissues. This results in a lower addictive potential and facilitates subjects to quit smoking [13].

The systemic clearance (CL) of nicotine is relatively high, around 0.8–1.5 L/min and depends on liver blood flow [7–11]. Nicotine is extensively metabolised in the liver to its major metabolite, cotinine. To a lesser extent, nicotine is also metabolised in the lung and kidney. Renal CL of unchanged nicotine (approximately 35–90 mL/min) accounts for 5–10% of total elimination. The reported elimination half-life of nicotine is on average 2 h [7], with substantial inter-individual variability (IIV).

Nicotine absorption is pH dependent [7]. In acidic environments, nicotine (pKa 7.9) is ionised and does not readily cross membranes whereas in basic environments nicotine is readily absorbed through oral, nasal and pulmonary mucous membranes. At physiological blood pH (7.4), only about 31% of nicotine is non-ionised. For this reason, to enhance absorption, some buccally administered dosage forms are buffered to a basic pH [7]. As a result of swallowing part of the administered dose, all buccal formulations also partially deliver the nicotine dose to the gastrointestinal tract. Swallowed nicotine is absorbed in the small intestine but undergoes extensive pre-systemic metabolism by the liver and has a relatively low (30–40%) bioavailability (F) [8–10, 12].

Nicotine is rapidly and efficiently absorbed through the skin, with a relatively high F of 68–82% [14, 15]. The nicotine concentration–time profiles after application of a nicotine patch appear to vary widely, depending on the type of patch used [16, 17]. When applying a patch daily for a 16-h period, nicotine stored in a shallow skin compartment is absorbed during the non-application night-time period, and a repeated-dose study over 6 days showed no accumulation of plasma nicotine [18].

Though several studies of intravenously administered nicotine have been reported, only a few model-based pharmacokinetic (PK) analyses were carried out [9, 11, 19, 20], in 10, 11, 24 and 40 subjects, respectively. In these studies, a two-stage approach was used to characterise nicotine pharmacokinetics through a two-compartment model in most subjects. Reports on the pharmacokinetics of orally ingested nicotine have mainly been based on model independent analyses. Levi et al. [21] conducted a population PK (PPK) analysis of data from 66 healthy subjects, where the well-stirred model for liver CL was incorporated, to characterise nicotine pharmacokinetics after oral administration. The PPK analysis of buccally administered nicotine in 702 healthy adult smokers was described by Marchand et al. [22], using a zero-order absorption process.

The PK properties of nicotine when administered buccally have been described previously for the sublingual tablet [23], inhaler [24], gum [25] and mouth spray [26]. However, no model-based PK analyses were presented for these studies.

Several PK studies with transdermal nicotine have been published [14–18], with limited model-based PK analyses. A population-based analysis was recently published; however, using only data during the washout after patch application [27].

During the development of different NRT formulations, a large volume of single- and repeated-dose nicotine PK data in healthy smoking volunteers was collected across a wide range of doses, routes of administration and formulations. We integrated data across a broad range of nicotine formulations and studies by developing predictive PPK models. This further increased our understanding of nicotine pharmacokinetics and its link with craving through exposure–response analyses, aiming to better understand and optimise the use of NRT [28]. Together, these models allow simulations of various dosing scenarios, e.g. for NRT combination treatment,

and simulations to inform the design and development of new improved NRT products.

2 Methods

2.1 Study Designs and Treatments

Data from 29 studies (Electronic Supplementary Material [ESM]) in 930 unique healthy smoking volunteers were included in the analysis. For each formulation, the dosing regimens and the number of trials, subjects, observations and doses are summarised in Table 1. Further details on study identification, study design, dosing regimens and sampling schedules for all studies are available in the ESM.

Microtablets were chewed before swallowing in one study (92NNBT005), while swallowed whole in another study (93NNBT007; see ESM). Mouth spray was administered as an oromucosal nicotine spray (Nicorette QuickMist, 1 mg/spray, McNeil AB) delivering 1 mg of nicotine per spray. Doses were varied by changing the number of sprays. The spray was administered straight into the mouth, except where otherwise indicated (see ESM). Chewing gums (Nicorette gum/Nicorette Freshmint/Freshfruit gum 2, 4 and 6 mg; McNeil AB) were chewed for 30 minutes, and chewing was timed to one chew every 2 seconds. Lozenges (Nicorette lozenge 2 and 4 mg; McNeil AB, and NiQuitine lozenge 2 and 4 mg; GlaxoSmithKline) were dissolved in the mouth without chewing. Inhalers (Nicorette Inhalator 10 and 15 mg; McNeil AB) were dosed by inhalation during 20 min for each dose. In the repeated-dose studies, inhalers were used for between one and four doses before being replaced.

In the nicotine patch studies, the patch (Nicorette patch 5–15 mg/16 h, Nicorette Invisipatch 10–25 mg/16 h; McNeil AB) was removed 16 h after application, except for study A6431108 where subjects received three daily doses, where patches were removed either at 16 h or at 24 h after application.

All studies were sponsored by McNeil AB and were conducted between 1993 and 2012 in accordance with the principles for human experimentation as defined in the Declaration of Helsinki and International Conference on Harmonization Good Clinical Practice guidelines. All studies were approved by the respective institutional review boards. Informed consent was obtained from each subject, given the investigational nature of the study (details in the ESM).

2.2 Bioanalytical Methods, Dataset Composition and Data Handling

Nicotine concentrations were assayed using a validated, single-step liquid–liquid extraction method and capillary gas chromatography coupled with either a nitrogen-sensitive detector [24] or chemical ionisation mass spectrometry (McNeil AB, data on file). The lower limit of quantification was 0.2–1 ng/mL. A single-step liquid-liquid extraction of nicotine was followed with a validated, capillary, gas chromatography-chemical ionisation mass spectrometry method, with ammonia as the reagent gas. Mass spectrometry detection was performed in the positive ionisation mode. The chromatographic system was multi-level calibrated via a linear regression function, with *N*-methylanabasine as the internal standard. The lower limit of quantification with the MS detector was 0.5 ng/mL.

For the chewing gum and patch studies, the actual dose for individual subjects and dosing occasions was calculated as the difference between the average nicotine content in the formulation batch and the residual nicotine after use of the individual formulations. Residual nicotine was assayed by reverse-phase high-performance liquid chromatography after extraction from the formulation. For the inhaler studies, the actual dose for individual subjects and dosing occasions was calculated based on the change in weight of the inhaler after each dosing period, using a calibration curve (McNeil AB, data on file).

Table 1 Summary of the number of trials, subjects, observations and doses for each formulation

Formulation	Dosing regimens	Trials	Subjects	Observations
Intravenous infusion	0.028 mg/kg in 10 min	4	80	1450
Oral microtablets	2 and 6 mg	2	26	392
Transdermal patch	5, 10, 15, 25 and 37 mg in 16 h	3	73	4469
Buccal formulations		21	774	39,705
Mouth spray	1, 2, 3 and 4 mg	6	201	9283
Chewing gum	2, 4 and 6 mg	14	512	17,287
Lozenge	2 and 4 mg	6	303	11,528
Inhaler	2 mg per 20 min of usage	3	58	1607

h hours, *min* minutes

2.3 Population Pharmacokinetic Model Development

An exploratory graphical analysis to identify possible starting models and to facilitate identification of potential outliers was conducted by plotting individual and mean profiles, also including dose-normalised concentrations, and inspecting them visually. The analyses of the plasma concentration data were performed using NONMEM Version 7.3.0 [29], supplemented with the Perl-speaks-NONMEM (PsN) toolkit version 4.7.0 [30], which was used to run execution, running visual predictive check (VPC) simulations and producing summaries. Further processing was conducted using R Version 3.4.1 [32] in accordance with appropriate regulatory guidelines [32, 33]. NONMEM runs were performed using the Intel Visual Fortran compiler, Version 11.1.056 (64 bit). NONMEM datasets were prepared using SAS 9.2 (SAS Institute Inc., Cary, NC, USA). Example files (script for data management and example source and output datasets) are included as ESM. Simulations were performed using Simulo 7.1 [34]. Analyses were performed on an Intel Xeon-based server running Linux (Centos release 5.5, 64 bit).

Models were compared using the objective function value, computed as −2 times the log-likelihood. NONMEM models were fitted using the first-order conditional estimation method with the INTERACTION option. Where the M3 method for modelling data below the validated limit of quantification (BQL) was used, the LAPLACIAN method was used instead.

An exponential model was used to describe the IIV and inter-occasion variability (IOV) of the model parameters. For parameters expected to stay within certain limits, e.g. between 0 and 1 for the fraction of the dose that was swallowed, IIV was applied on the logit scale. Correlations between random-effect parameters were also investigated. The residual error was modelled using a combined additive and proportional error model.

Attempts at fitting joint models combining the transdermal, oral or buccal data with the iv data, using both the first-order conditional estimation and the stochastic approximation expectation-maximisation methods, or using a Bayesian approach with the iv model parameters as a prior knowledge for the other models were unsuccessful. To avoid bias, the parameters of the disposition model (CL, inter-compartmental flows and volume [Vn]) were fixed to the estimates from the iv model. A visual representation of the ultimately applied structural models for all the routes of administration is outlined in Fig. 1.

2.3.1 Intravenous Population Pharmacokinetic Model

As indicated by the individual plots in Fig. 2, open two-, three- and four-compartment models were explored for describing the nicotine pharmacokinetics after iv dosing. In three of the studies, the majority of samples collected 24 h after dosing were BQL (173 observation, 12% of the data). Modelling of the data by excluding BQL data resulted in a clear bias, fitting the detectable observations well, but predicting concentrations well above the limit of quantification for this last observation. To appropriately account for the BQL data, the M3 method, as described by Bergstrand and Karlsson [35] was used. This method is based on simultaneous modelling of continuous and categorical data, where the BQL observations are treated as categorical data. The likelihood for BQL observations is maximised with respect to the model parameters and the likelihood for an observation is taken to be the likelihood that it is indeed BQL. For the transdermal, buccal and oral data, however, the M3 method did not lead to successful termination of the fitting and, consequently, the BQL data were excluded from the analysis.

As nicotine has a high hepatic extraction ratio, its systemic CL is to a large extent driven by liver blood flow. Allometric scaling by body weight (WT/70) was explored for the CL and V_n parameters. The allometric exponent for CL and inter-compartmental flows was fixed to 0.75, and to 1.0 for V_n [36].

2.3.2 Residual Background Nicotine

To minimise the influence of residual nicotine from smoking, washout periods were implemented in the studies, varying from 12 h (transdermal, oral and buccal) to 36 h (iv) before the first dose in each period. However, detectable baseline nicotine concentrations were found in many subjects at the time of dosing. For instance, in two studies (96NNIV004 and 96NNIV005), where several pre-dose samples were taken, plasma concentrations decreased during the washout period in a manner similar to the terminal phase after dosing (Fig. 2). The residual nicotine concentration in plasma was treated as part of the model. For this, a virtual bolus dose into the central compartment was assumed to be given at the start of the washout period, and the amount in this dosing compartment was estimated by fixing the dose to 1, and estimating the F of this dose, $F_{smoking}$. Inter-individual variability and IOV, when more than one dosing period occurred, were applied to $F_{smoking}$, to account for the variability in smoking between and within individuals. The decay after this dose was estimated using the same model as that describing the pharmacokinetics after iv administration, using individual estimates for the subject in question.

2.3.3 Oral Population Pharmacokinetic Model

First-order absorption, with and without a lag time or delay via transit compartments, was explored to characterise the nicotine gastrointestinal absorption. Exploration showed a
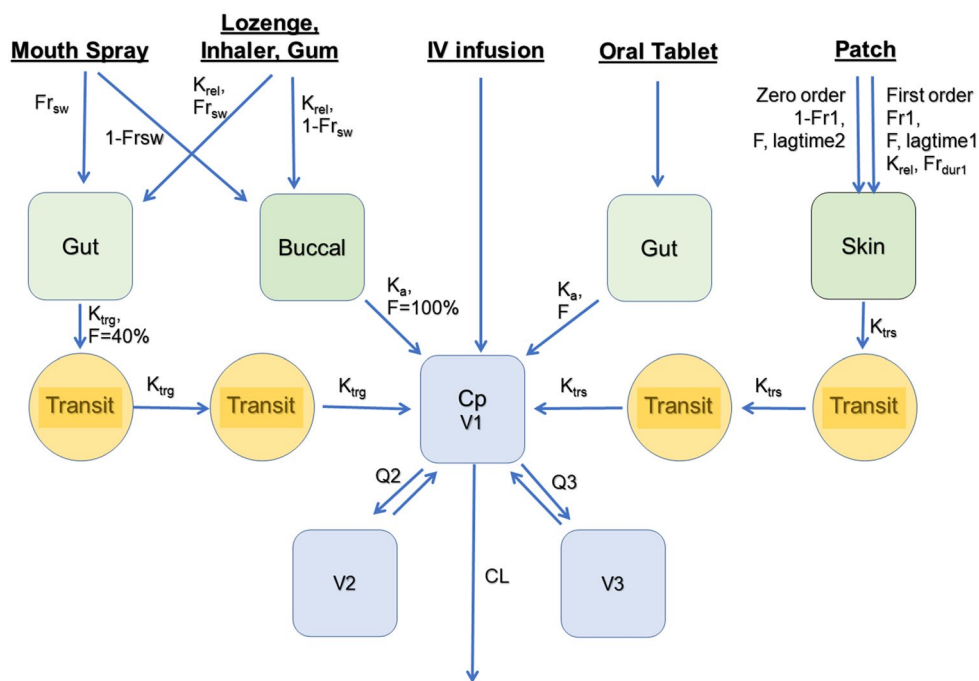
Fig. 1 Structure of the intravenous (iv), transdermal and buccal models. After iv administration, the pharmacokinetics are described by the disposition parameters: clearance (CL), $Q2$, $Q3$, $V1$, $V2$ and $V3$. For the other models, these parameters were fixed to estimates obtained from fitting the iv data. Gum, lozenge and inhaler release nicotine with zero- or first-order rates, while the mouth spray is delivered as a bolus. A fraction of the dose $(1 − Fr_{sw})$ is absorbed directly from the buccal cavity with a bioavailability of 100% and a first-order absorption rate constant, K_a. The remainder, Fr_{sw}, is swal-lowed, where it is absorbed with a bioavailability of 40%, and delayed absorption implemented using two transit compartments, with a transit rate constant, K_{trg}. Release from the patch is through two parallel pathways. A fraction Fr1 of the dose is released through a first-order pathway, with a release rate, K_{rel}. The duration of this first-order process is limited to $Fr_{dur1} \times 16$ h (application duration). The remainder $(1 − Fr1)$ is delivered through a zero-order pathway. F is the absolute transdermal bioavailability and K_{trs} is the transit rate constant

clear difference between the pharmacokinetics in the two studies included in the analysis, and separate parameters and absorption models were explored by study. Graphically exploring the repeated-dose oral data, the accumulation appeared to slow down during part of the day, even leading to a temporary decrease in trough concentrations (Fig. 4). This was explored in the model as time-dependent changes in CL or F, using different parameterisations (step-change, Bateman function, sigmoidal change).

2.3.4 Buccal Population Pharmacokinetic Model

Data from the different buccal formulations (Fig. 6) suggested that an initial rapid peak within 10 min was followed by a secondary peak after 1–3 h, with large variability in the absorption profiles. Therefore, parallel absorption pathways were explored, intended to represent the oromucosal absorption, and the gastrointestinal absorption after swallowing part of the dose. The fraction of the dose that went through the second pathway, i.e. being swallowed (Fr_{sw}), was estimated from the available data. The part of the dose that was not swallowed was assumed to be absorbed through the

oromucosal pathway with a F of 100%, while for all buccal formulations the same estimate of F derived from the oral data was used for the absorption from the gut. Consequently, for the buccal formulations, the same model structure (Fig. 1) was used for the absorption of nicotine released from all formulations, while the release from the formulation was varied according to formulation properties.

After mouth spray, the dose was assumed to be immediately delivered partially into the buccal cavity and partially into the gut, as described by the fraction Fr_{sw}. For the chewing gums, zero- and first-order release, stopping at the end of the 0.5-h chewing period, were explored. The first-order release rate (K_{rel}) was calculated as

$$K_{rel} = -\log\left(1 - \frac{ADOSE}{NDOSE}\right)/0.5, \qquad (1)$$

where NDOSE is the nominal dose and ADOSE is the individual amount released calculated from residual nicotine in the gum. This ensures the correct amount is released during the 0.5-h chewing period. For the lozenge formulations, a first-order release rate constant was estimated. Finally, for the inhaled formulations, a zero-order release rate was
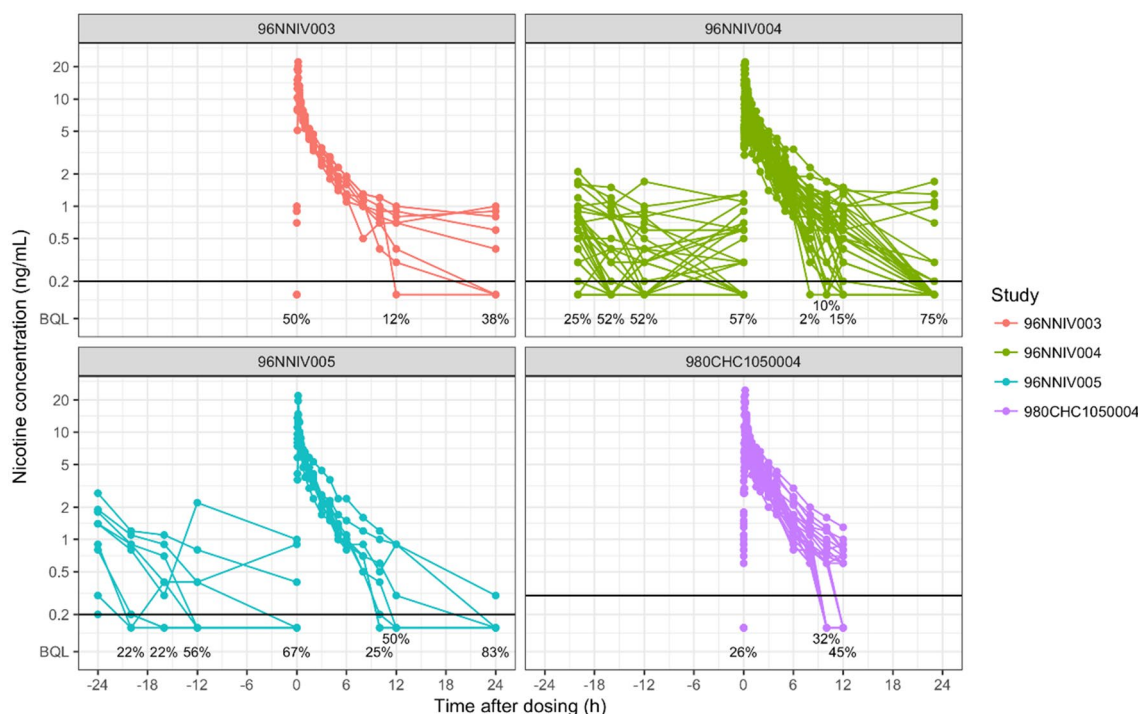
Fig. 2 Individual nicotine concentrations after intravenous (iv) administration. Individual nicotine concentration curves after iv administration. Log-linear plots, by study. Concentrations at times less than zero indicate residual nicotine from pre-study smoking. Horizontal lines indicate the limit of quantification, and concentrations below this limit are plotted as 0.1. Numbers at the bottom of each graph indicate the fraction of observations that are below the limit of quantification (BQL) at each timepoint

assumed for the dose being estimated from the residual weight of the inhalers, and the duration being that of the inhalation period, 20 min.

Effects of formulation on lag time, Fr_{sw}, and the oromucosal first-order absorption rate constant, K_a, were explored. The effect of nicotine dose on Fr_{sw} was also explored, as was the effect of the site of administration of the mouth spray on K_a. Similar to the oral dosing, graphical exploration of the repeated-dose data for all the buccal formulations indicated a change in CL or F over time. Similar models as for the oral data were tested to account for this aspect.

2.3.5 Transdermal Population Pharmacokinetic Model

The release of nicotine from the patch was empirically described by two parallel-release mechanisms, followed by a joint absorption pathway through the skin. One release pathway followed zero-order kinetics, lasting until patch removal. The other release pathway followed first-order kinetics, and finished at a time before patch removal, which was estimated as a fraction of 16 h, the usual time of patch removal. The fraction going through the first-order pathway, Fr_1, was estimated. After release from the patch, nicotine absorption was modelled as a series of transit compartments.

2.4 Model Evaluation and Model-Based Simulations

In addition to goodness-of-fit plots to evaluate the predictive performance of the PK models, VPCs, where 5th, 50th and 95th percentiles of binned observations were compared to the simulated percentiles with 95% confidence intervals, were performed on the final model parameter estimates [37]. The PPK models developed were used to simulate and compare PK profiles from the buccal formulations evaluated.

3 Results

3.1 Analysis Data Set and Population

For the iv dataset, 173 measurements (12% of the data) that were reported as BQL were retained in the dataset and successfully analysed using the M3 method [35] to avoid potential bias. Across the transdermal, buccal and oral data, however, a total of 2258 BQL values (5% of the data) were excluded from the analysis as the M3 method did not lead to successful termination of the fitting. After graphical evaluation, one subject-period profile (18 observations) after administration of mouth spray was excluded from the analysis as an outlier.

Table 2 Summary of subject demographics

	IV	Oral	Gum	Mouth spray	Lozenge	Inhaler	Transdermal
N (%)	80 (6.4)	26 (2.1)	512 (40.9)	201 (16.0)	303 (24.2)	58 (4.6)	73 (5.8)
Age, years							
Mean (CV%)	42.0 (43.7)	36.6 (20.7)	28.9 (31.3)	29.9 (29.0)	30.7 (29.7)	31.9 (27.7)	27.2 (28.6)
Median (range)	36.0 (20.0–76.0)	38.0 (24.0–47.0)	26.0 (18.0–50.0)	27.0 (18.0–50.0)	28.0 (18.0–50.0)	29.0 (22.0–49.0)	24.0 (19.0–50.0)
Weight, kg							
Mean (CV%)	71.4 (16.4)	67.4 (21.9)	71.8 (15.3)	73.5 (15.5)	73.6 (14.6)	69.6 (19.9)	72.1 (17.3)
Median (range)	72.9 (49.0–99.0)	62.5 (44.0–105.0)	71.5 (40.6–108.0)	72.6 (49.4–105.6)	72.8 (52.2–105.0)	71.0 (43.0–101.0)	71.2 (43.2–112.8)
BMI							
Mean (CV%)	23.4 (12.1)	22.2 (12.7)	23.5 (11.8)	23.7 (12.4)	23.9 (11.3)	22.9 (14.2)	22.9 (11.9)
Median (range)	23.2 (17.6–31.9)	22.1 (18.1–31.0)	23.1 (17.8–30.7)	23.3 (17.5–29.9)	23.6 (18.3–29.9)	22.4 (17.7–31.2)	22.3 (18.2–30.0)
Smoking years							
Mean (CV%)	NA (NA)	NA (NA)	13.1 (66.6)	13.5 (64.1)	14.6 (60.8)	10.8 (70.1)	10.9 (71.9)
Median (range)	NA (NA–NA)	NA (NA–NA)	11.0 (1.0–38.0)	12.0 (1.0–38.0)	13.0 (2.0–38.0)	8.0 (5.0–33.0)	8.0 (1.0–37.0)
Number of cigarettes per day							
Mean (CV%)	NA (NA)	NA (NA)	18.6 (19.3)	18.7 (20.1)	18.8 (19.7)	15.9 (22.3)	17.5 (15.3)
Median (range)	NA (NA–NA)	NA (NA–NA)	20.0 (10.0–30.0)	20.0 (10.0–35.0)	20.0 (10.0–30.0)	16.0 (10.0–20.0)	18.0 (12.0–25.0)
Sex (%)							
Male	43 (53.8)	12 (46.2)	266 (52.0)	112 (55.7)	160 (52.8)	27 (46.6)	45 (61.6)
Female	37 (46.2)	14 (53.8)	246 (48.0)	89 (44.3)	143 (47.2)	31 (53.4)	28 (38.4)
Race (%)							
Missing	0 (0.0)	26 (100.0)	6 (1.2)	0 (0.0)	104 (34.3)	0 (0.0)	0 (0.0)
White	78 (97.5)	0 (0.0)	497 (97.1)	199 (99.0)	197 (65.0)	57 (98.3)	73 (100.0)
Asian or Pacific Islander	2 (2.5)	0 (0.0)	3 (0.6)	2 (1.0)	0 (0.0)	0 (0.0)	0 (0.0)
Black or African American	0 (0.0)	0 (0.0)	3 (0.6)	0 (0.0)	1 (0.3)	0 (0.0)	0 (0.0)
Other	0 (0.0)	0 (0.0)	3 (0.6)	0 (0.0)	1 (0.3)	1 (1.7)	0 (0.0)

Percentages shown in parentheses. Some subjects have received more than one formulation

BMI body mass index, *CV* coefficient of variation, *IV* intravenous, *NA* not available

Demographic characteristics are summarised in Table 2. Demographics are similar for the different routes of administration, with age slightly higher in the iv and oral studies.

3.2 Intravenous Model

Individual PK profiles are presented in Fig. 2. Considerable variability between subjects is observed.

The pharmacokinetics of nicotine after iv dosing were found to be well described by a three-compartment model where CL and V_n were allometrically scaled for body weight to a 70-kg typical individual. A two-compartment model was significantly worse (objective function value difference 1083.213; $p < 0.001$), and a four-compartment model could not be estimated. Pre-dose concentrations could be well described using a bolus dose at the start of the washout. Exploration using the iv model showed that within 1–2 h after dosing, the nicotine profiles of a bolus dose, an infusion and a repeated administration could be scaled to become nearly identical, indicating that the use of a virtual bolus dose is a valid approximation to deal with this nuisance parameter. The VPC in Fig. 3 shows good agreement between predicted concentrations and observations, both for the pre-dose washout period and post-dose, though there is an indication that the variability may be somewhat overestimated. Additionally, there is good agreement between the predicted and observed proportions of observations that are BQL, over time.
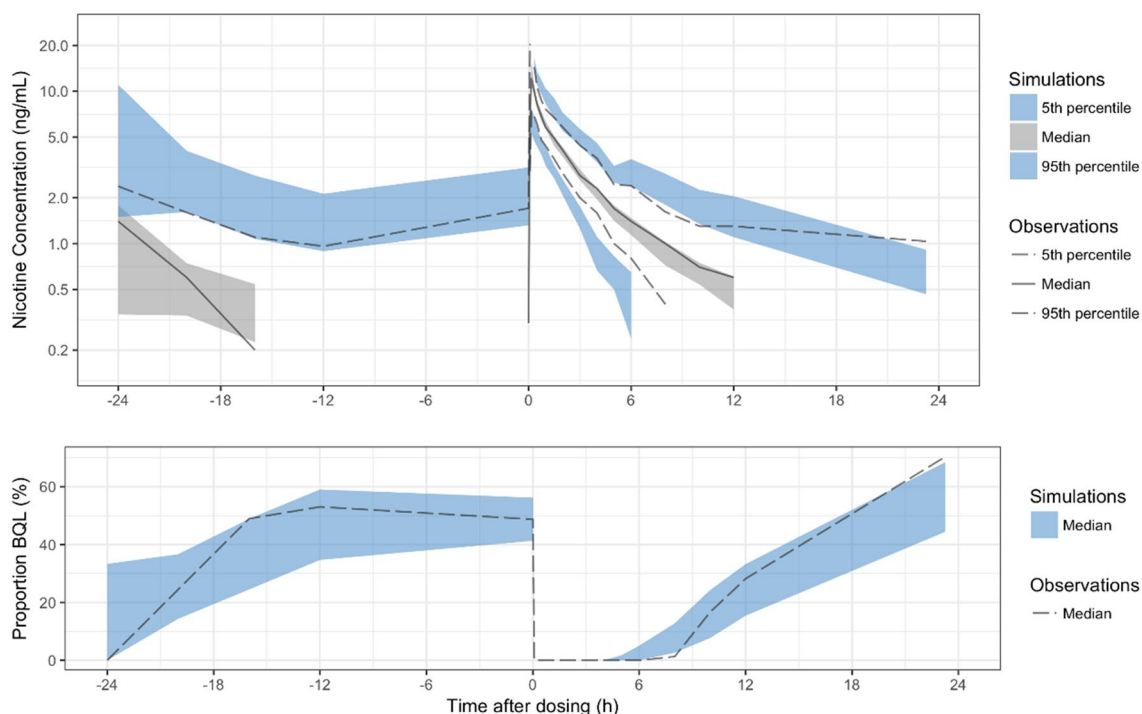
Fig. 3 Visual predictive check for the final intravenous model. The top panel shows concentrations above below the limit of quantification (BQL). Lines show observed values, the solid line is the median, and the dashed lines are the 5th and 95th percentiles of observed concentrations. Areas indicate 95% confidence intervals based on the model. Grey for median, blue for 5th and 95th percentiles. The bottom panel shows the observed (line), and 95% confidence intervals (area) for the fraction of observations that is BQL vs time

The parameter estimates for the iv model are presented in Table 3. Fixed-effects parameters were estimated with fairly good precision (relative standard error < 30%). The IIV was moderate to high, which is in accordance with the wide range of terminal half-lives observed in the data (Fig. 2). The estimated half-lives (fractions of total area under the curve) associated with the rapid, intermediate and slowest disposition phase were 7 min (0.04), 57 min (0.36) and 4.5 h (0.61), respectively.

3.3 Oral Model

As indicated by the individual plots in Fig. 4, the pharmacokinetics after oral dosing show a large variability from subject to subject. The parameter estimates for the oral PK model are presented in Table 4. The absorption was found to be relatively fast in study 92NNBT005 (ESM) and was best described by a first-order absorption with a K_a of 1.55 h^{-1} and an absolute F of 40%. In study 93NNBT007 (ESM), absorption was slower and was best described by a series of three transit compartments with a transit rate constant (K_{tr}) of 3.6 h^{-1}, corresponding to a mean transit time of 1.1 h. The absolute F was estimated to be lower, 22%.

In the repeated-dose study (92NNBT005), a decrease in concentrations could be observed between 6 and 8 h. This

was best described using time-varying CL, based on the following empirical equation:

$$P = P_{bl} \times \left(1 + E_{max} \times \frac{\text{Time}^{\text{pow}}}{\text{Start}^{\text{pow}} + \text{Time}^{\text{pow}}} - \frac{\text{Time}^{\text{pow}}}{(\text{Start} + \text{Duration})^{\text{pow}} + \text{Time}^{\text{pow}}} \right),$$

(2)

where P is the time-varying parameter (in this case, CL), P_{bl} is the parameter at baseline, E_{max} is the maximal change in the parameter, time is the time since the first dose in the treatment period, Start is the time of 50% effect onset, Duration is the duration of the effect, and pow is a factor determining the rate of the onset and offset. The maximal increase in CL was estimated at 77%, starting around 5.3 h and lasting for 1.9 h. A time effect on the F gave a very similar fit to having the effect on CL, but with a moderately higher objective function.

The final model had exponential IIV on F, K_{tr}, duration and pre-washout nicotine dose. The VPC in Fig. 5 shows good agreement between predicted concentrations and observations, including the decrease in concentrations during the day in the repeated-dose study.

Table 3 Parameters of the final intravenous model

Parameter	Estimate	RSE (%)[a]	90% CI[b]	Shr. (%)[d]
Fixed-effects parameters				
CL (L/h)	67.4	4.80	62.1 to 72.7	–
$V1$ (L)	117	13.3	91.8 to 143	–
$Q2$ (L/h)	38.6	5.96	34.8 to 42.4	–
$V2$ (L)	130	25.0	76.8 to 184	–
$Q3$ (L/h)	216	5.45	197 to 236	–
$V3$ (L)	53.4	12.3	42.6 to 64.2	–
Pre-washout nicotine dose (mg)	4.90	11.9	3.94 to 5.86	–
Random-effects parameters				
IIV CL (CV%)[c]	27.0	19.4	22.2 to 31.2	3.15
IIV V1 (CV%)[c]	68.1	29.7	46.4 to 87.3	0.571
Covariance $V1/V3$	− 0.231	52.8	− 0.431 to − 0.0303	–
IIV $V3$ (CV%)[c]	75.4	30.0	50.6 to 98	3.97
Covariance $V2/V3$	0.553	26.0	0.317 to 0.789	–
IIV $V2$ (CV%)[c]	230	24.1	142 to 346	14.8
IIV pre washout nicotine dose (CV%)[c]	82.5	28.3	56.5 to 107	25.4
Residual variability				
Proportional residual error	0.0926	2.01	0.0896 to 0.0957	12.8
Additive residual error (ng/mL)	0.212	2.42	0.204 to 0.221	–

CI confidence interval, *CL* clearance, *CV* coefficient of variation, *IIV* inter-individual variability *(R)SE* (relative) standard error, *Shr.* shrinkage

[a]RSE on variance scale for variability estimates

[b]Asymptotic confidence interval derived from NONMEM standard errors

[c]CV = $100 \times \mathrm{sqrt}(\exp(\mathrm{variance}) - 1)$

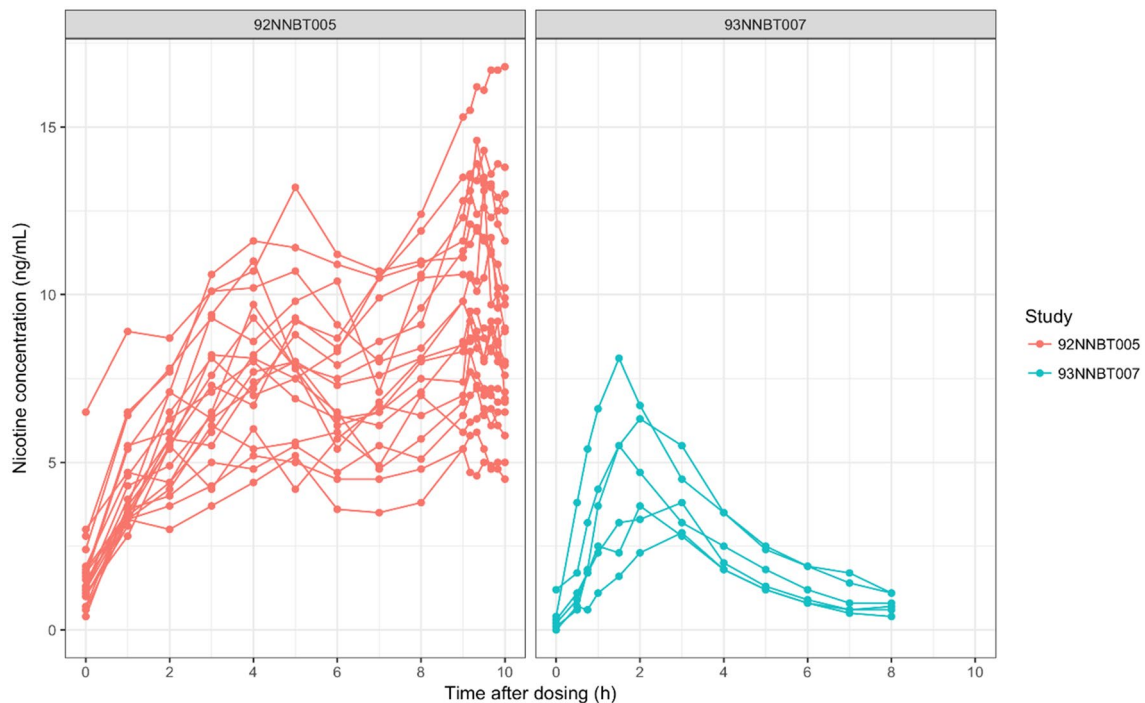[d]Epsilon shrinkage is the overall shrinkage for related elements of the residual error

Fig. 4 Individual nicotine concentrations after oral administration, by study

Table 4 Parameters of the final oral model

Parameter	Estimate	RSE (%)[a]	90% CI[b]	Shr. (%)[d]
Fixed-effects parameters				
K_a (h^{-1})	1.55	22.5	0.978 to 2.12	–
F study 92NNBT005 (%)	39.5	10.2	32.8 to 46.1	–
F study 93NNBT007 (%)	22.3	21.5	14.4 to 30.1	–
K_{tr} study 93NNBT007 (h^{-1})	3.60	47.8	0.771 to 6.42	–
Start (h)	5.29	5.30	4.83 to 5.75	–
Duration (h)	1.92	40.3	0.646 to 3.19	–
E_{max} (%)	77.3	32.8	35.6 to 119	–
pow	12.3	37.4	4.74 to 19.9	–
Pre-washout nicotine dose (mg)	4.92	24.7	2.92 to 6.93	–
Random-effects parameters				
IIV F (CV%)[c]	22.6	93.5	0 to 36.7	23.9
IIV K_{tr} (CV%)[c]	45.2	147	0 to 94	57.1
IIV pre-washout nicotine dose (CV%)[c]	91.7	53.8	27 to 147	19.5
IIV duration (CV%)[c]	63.7	73.9	0 to 106	32.7
Residual variability				
Proportional residual error (%)	9.87	9.18	8.38 to 11.4	12.1
Additive residual error (ng/mL)	0.162	64.7	− 0.0103 to 0.335	–

CI confidence interval, *CV* coefficient of variation, *F* bioavailability, *IIV* inter-individual variability, K_a absorption rate constant, K_{tr} transit rate constant, *(R)SE* (relative) standard error, *Shr.* shrinkage

[a]RSE on variance scale for variability estimates

[b]Asymptotic confidence interval derived from NONMEM standard errors

[c]CV = 100 × sqrt(exp(variance) − 1)

[d]Epsilon shrinkage is the overall shrinkage for related elements of the residual error
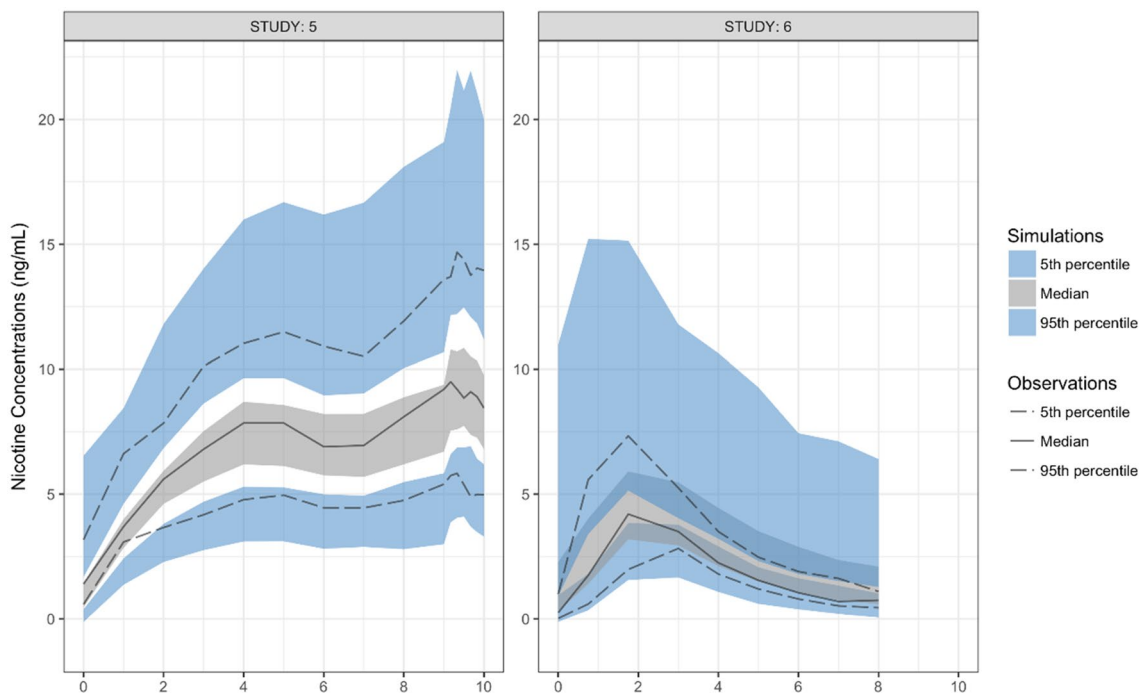

Fig. 5 Visual predictive check for the final oral model. Study 5—Study 92NNBT005, Study 6—Study 93NNBT007. Lines show observed values, the solid line is the median, and the dashed line is the 5th and 95th percentiles of observed concentrations. Areas indicate 95% confidence intervals based on the model. Grey for median and blue for 5th and 95th percentiles

3.4 Buccal Models

As exemplified by selected individual data for the different buccal formulations from four different studies (Fig. 6), there was a large variability in absorption, often with an initial rapid peak within 10 min followed by a secondary peak after 1–3 h. A visual representation of the applied structural model for buccal formulations is outlined in Fig. 1.

The parameter estimates for the buccal PK models are presented in Table 5. Mouth spray is dosed directly into the buccal and gut compartments as a bolus, while chewing gum and lozenges release nicotine with a first-order rate constant, K_{rel}, calculated to be on average 2.8 h^{-1} for chewing gum and estimated at 6.4 h^{-1} for lozenges. Release of nicotine from inhalers is described by a zero-order process, where on average 2.0 mg of nicotine is released over the 20-min inhalation period. After release from the different formulations, a fraction of the dose (Fr_{sw}) is swallowed, and is absorbed through two transit compartments, with a K_{tr} between 3.5 h^{-1} and 5.5 h^{-1} corresponding to a mean transit time of 33–51 min

and an oral F fixed to 40%, based on the estimate from the oral model. After a brief lag time, the remainder $(1 - Fr_{sw})$ is absorbed oromucosally through a first-order process. The estimated Fr_{sw} was lowest for chewing gum, followed by the mouth spray, inhaler and lozenge. The absorption rate was fastest for Nicorette classic chewing gum, followed by mouth spray, lozenge, Freshmint/Freshfruit chewing gum, and, with a much slower K_a, inhaler. After sublingual administration of the mouth spray, the absorption was markedly faster compared with buccal administration. Nicorette lozenges were associated with a higher fraction swallowed than NiQuitin lozenges. Increasing doses were associated with an increase in Fr_{sw} (mouth spray, lozenge) and an increase in K_a (chewing gum).

On repeat dosing, exposure increased less than expected. As for the oral data, these were best described using Eq. (2), with average increases in CL of around 30% (Fig. 7) for the inhaler, lozenge and mouth spray. For chewing gum, the change in exposure was best described by a decrease in F of 75%.
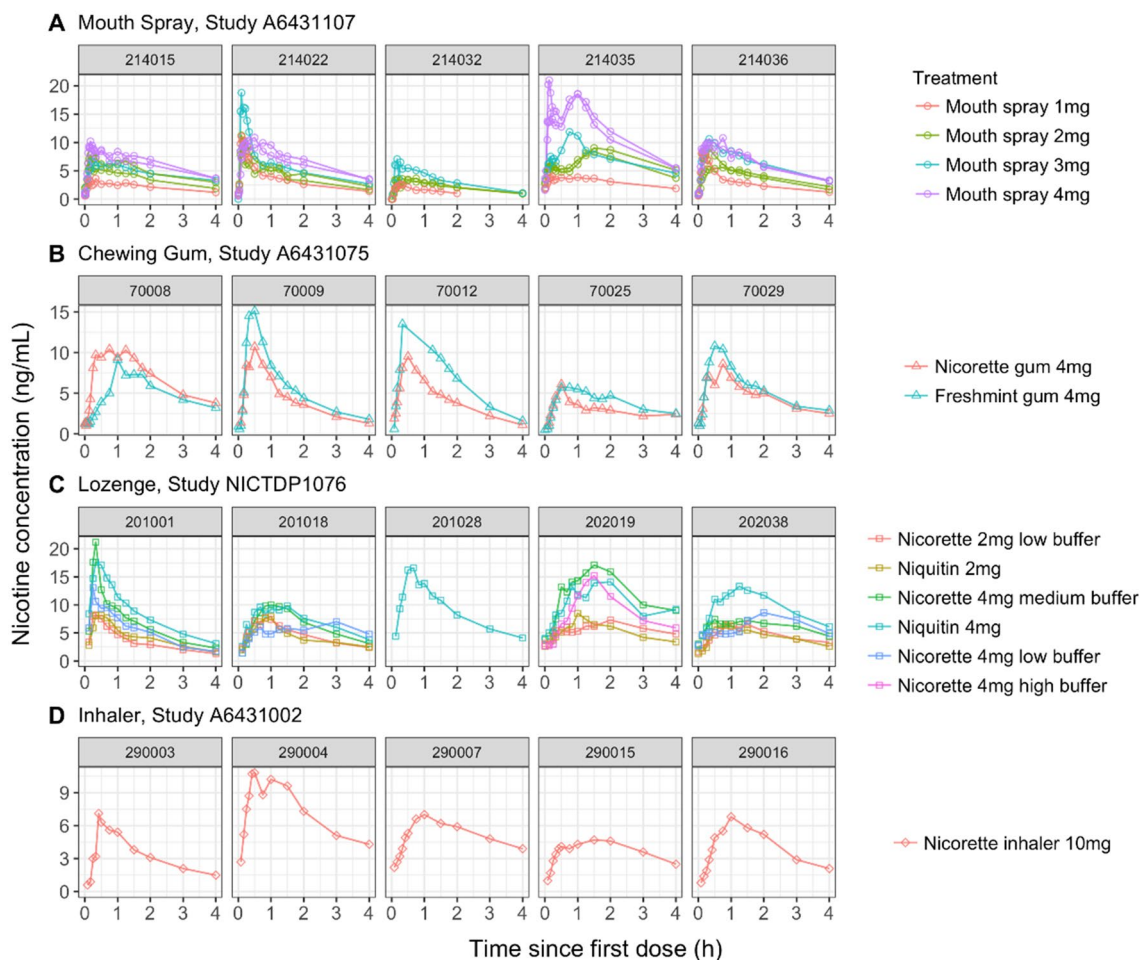

Fig. 6 Selected individual concentration–time profiles during the first 4 h after dosing of four different buccal formulations. Randomly selected profiles from four single-dose studies: **a** mouth spray, Study A6431107; **b** chewing gum, study A6431075; **c** Lozenge, Study NICTDP1076; and **d** inhaler, Study A6431002

Table 5 Parameters of final buccal models

	Mouth spray			Chewing gum			Lozenge			Inhaler		
	Estimate	RSE (%)[a]	Shrinkage (%)[b]	Estimate	RSE (%)[a]	Shrinkage (%)[b]	Estimate	RSE (%)[a]	Shrinkage (%)[b]	Estimate	RSE (%)[a]	Shrinkage (%)[b]
Fixed-effects parameters												
K_{rel} (h⁻¹)	NA			2.8	Calculated		6.41	4.9				
Lag time (h)	0.0230	2.4		0.0531	0.6		0.0437	3.6				
K_a (h⁻¹)	15.9/86.0[c]	3.4, 17		26.5/9.29[d]	1.0, 0.4		11.6	6.7		0.753	6.0	
Fr_{sw} (%)	60.6/64.6[e]	1.2		54.7	0.2		64.0/68.8[e]	1.3		66.9	4.5	
K_{trg} (h⁻¹)	3.70	3.0		5.53	0.6		3.54	2.3		5.26	7.3	
E_{max} (%)	35.7	10		−75.2	0.1		54.4	15		23.2	14	
Start (h)	3.37	5.4		0.636	0.6		4.86	8.4		2.06	2.6	
Duration (h)	8.78	12		13.9	0.3		20.2	20		4.47	7.2	
pow	4.82	11		6.75	0.4		9.88	9.9		80 (fixed)		
Dose on K_a[f]				0.507	2.8							
Nicorette on Fr_{sw}[g]							0.412	12		66.0	21	
F increase, Study 97NNIN024 (%)										7.31	11	
Pre-washout nicotine dose (mg)	4.84	7.6		6.93	0.4		5.44	5.8				
Random-effects parameters												
IIV lag time (CV%)	22.0	9.4	24	37.5	8.9	22	32.3	16	37			
IIV Fbuccal (CV%)							23.4	25	42			
IIV Foral (CV%)	60.0	14	21	71.3	6.9	14	61.0	13	21	35.1	66	40
IIV K_a (CV%)							94.4	16	32	29.1	44	37
IIV E_{max} (CV%)				366	22	66	43.2	24	48	60.9	56	30
IIV start (CV%)				56.3	16	66						
IIV duration (CV%)	84.9	46	62	84.3	22	62	73.1	53	66	29.6	73	65
IIV Pre-washout nicotine dose (CV%)	81.5	13	24	85.5	7.0	25	61.4	16	29	38.7	65	41
IOV K_{rel} (CV%)							68.7	9.3	45			
IOV K_a (CV%)	96.0											
IOV Fr_{sw} (CV%)	0.294			1.04	4.1	27	0.245	9.0	42	0.483	37	28
IOV K_{tr} (CV%)	65.1						56.9	7.0	37	52.8	32	23
IOV pre-washout nicotine dose (CV%)	50.7			42.2	5.8	46	43.1	5.8	47	24.4	48	47
Residual variability												
Proportional residual error (%)	10.1	0.4	14	10.4	0.2	11	10.7	0.4	15	7.61	2.0	14

Table 5 (continued)

	Mouth spray			Chewing gum			Lozenge			Inhaler		
	Estimate	RSE (%)[a]	Shrinkage (%)[b]	Estimate	RSE (%)[a]	Shrinkage (%)[b]	Estimate	RSE (%)[a]	Shrinkage (%)[b]	Estimate	RSE (%)[a]	Shrinkage (%)[b]
Additive residual error (ng/mL)	0.136	2.6		0.157	0.5		0.0851	3.6		0.179	5.8	

IOV Fr_{sw} on logit scale

CV coefficient of variation, $CV\% = 100 \times$ sqrt(exp(variance) – 1), F bioavailability, IIV inter-individual variability, IOV inter-occasion variability, IV intravenous, Ka absorption rate constant, $Krel$ first-order release rate, K_{tr} transit rate constant, $(R)SE$ (relative) standard error

[a] RSE on variance scale for variability estimates

[b] Epsilon shrinkage is the overall shrinkage for related elements of the residual error

[c] K_a after buccal and sublingual administration, respectively

[d] K_a after 3 mg of Nicorette classic and 2 mg of Freshmint, respectively

[e] Fr_{sw} after 2 and 4 mg, respectively

[f] $K_a = K_{a2mg} + (1/NDOSE)^{0.507}$

[g] Additive on logit scale

Inter-individual variability and IOV was applied across many of the parameters, as shown in Table 5. Both IIV and IOV were fairly high for many of the parameters.

Figure 8 shows VPCs of the single- and repeated-dose data. The absorption is captured well for all formulations, though it is slightly too slow for lozenge. The accumulation on repeat dosing is also well described. For chewing gum, the variability appears somewhat over-estimated. Goodness-of-fit plots for all models can be found in the ESM.

3.5 Transdermal Model

There was a short delay after administration of a patch, after which concentrations rose to a peak around 10 h after administration, see Fig. 9. Concentrations then decreased during the remainder of the administration period. After the patch was removed, normally at 16 h after application, concentrations decayed more rapidly. When the patch was kept on for 24 h, the trough exposure increased, but there was not a large difference in peak exposure. The Invisipatch appeared to have a slightly delayed absorption, though it is otherwise similar to the Nicorette patch.

The structure of the final transdermal model is presented in Fig. 1. The parameter estimates for the transdermal PK model are presented in Table 6. For Nicorette patches, a fraction (Fr_1) equaling 40% of the dose is released through a slow first-order pathway, with a rate constant K_{rel}, estimated at 0.15 h^{-1}. This process lasts until 7.1 h after the patch application. The remainder of the dose is released through a zero-order pathway, starting 4.1 h after dosing and ending when the patch is removed. To make sure all release stopped when the patch is removed, the duration of the first-order process was modelled as a fraction (Fr_{dur1}) of the shortest application time, 16 h.

For Invisipatch, 72% is released through a first-order pathway, also with a K_{rel} of 0.15 h^{-1}, which starts after a lag time of 0.53 hours and lasts until 15 h after patch application. The remainder of the dose is released through a zero-order pathway, starting 4.1 h after dosing and ending when the patch is removed.

After nicotine release from both patch types, its absorption through the skin is best described by three transit compartments, with a transit rate constant of 3.6 h^{-1}, corresponding to a mean transit time of 1.1 h. The estimated transdermal F of nicotine released from the patch is 76%. On repeat dosing, accumulation was somewhat lower than expected. This was best described by a 12% increase in CL starting 24 h after the first dose.

Figure 10 shows a VPC of the single- and repeated-dose data. There is a tendency to under-predict the peak, at approximately 10 h, and there is also some under-prediction after a 24-h application. The rest of the nicotine plasma concentration
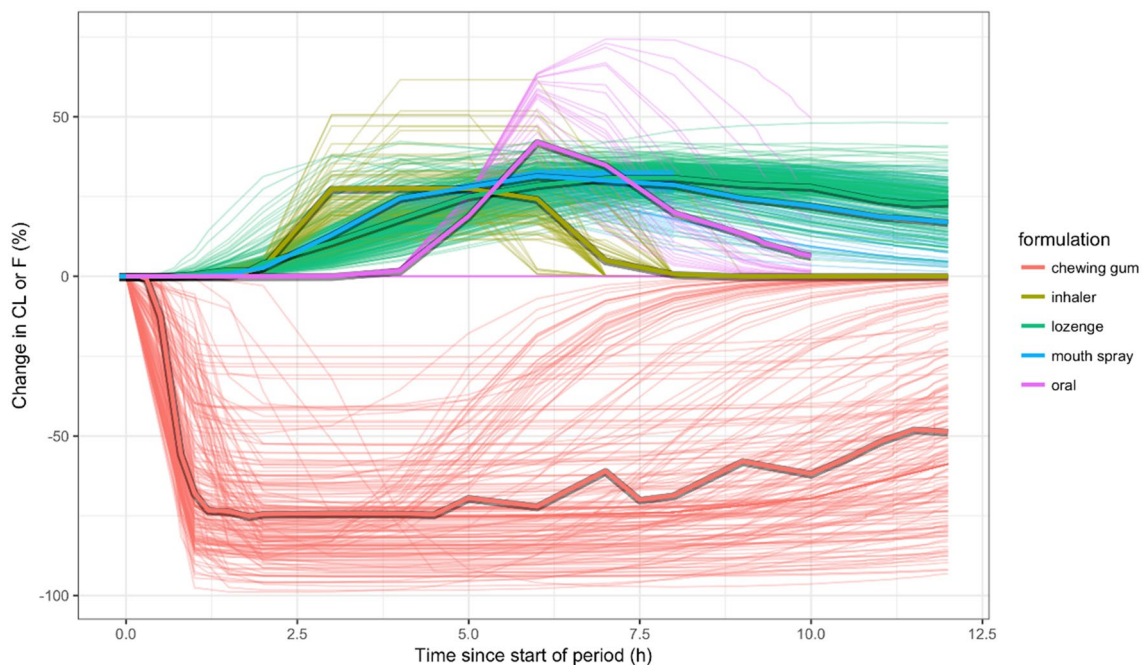
Fig. 7 Changes in clearance (CL) and bioavailability (*F*) over time. Model-predicted individual (thin lines) and mean (thick lines) increases in CL (oral dose, mouth spray, inhaler and lozenge) and decrease in *F* (chewing gum) of nicotine over time
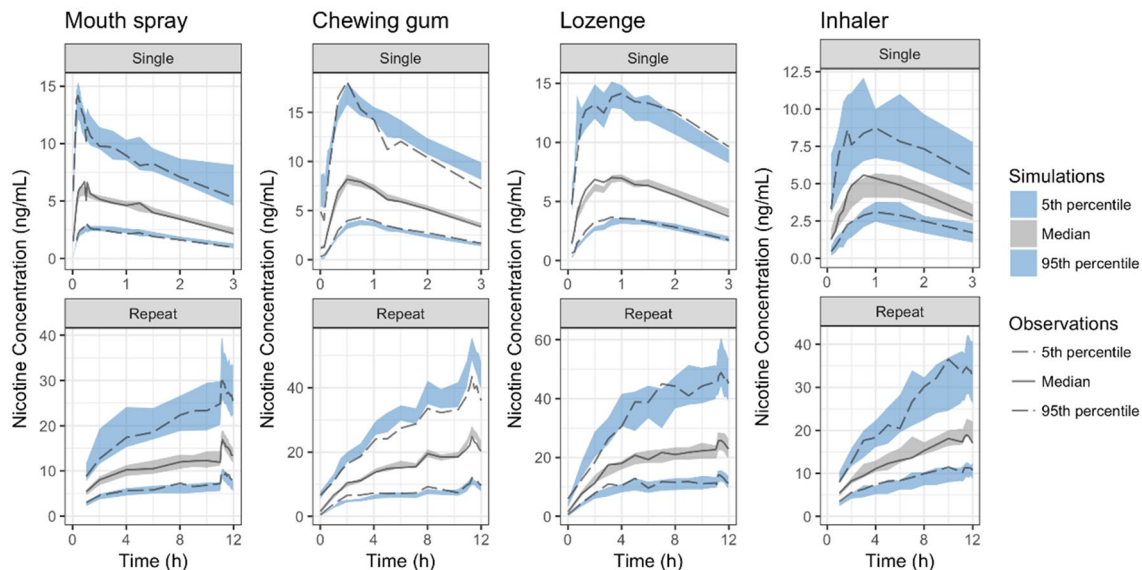

Fig. 8 Prediction-corrected visual predictive checks of final buccal nicotine models after single and repeat dosing. Single-dose data show first 3 h after administration. From right to left: mouth spray, chewing gum, lozenge, inhaler. The solid line is the median, and the dashed lines are the 5th and 95th percentiles of observed concentrations. Areas indicate 95% confidence intervals based on the model, grey for median, blue for 5th and 95th percentiles.

profile, including its variability, appears to be described fairly well by the model. Example NONMEM model output files for all models are included in the ESM.

3.6 Simulation Results

As an example of applications of the PPK models, simulations comparing the pharmacokinetics after administration of the different buccal formulations are shown in Fig. 11. Likewise,
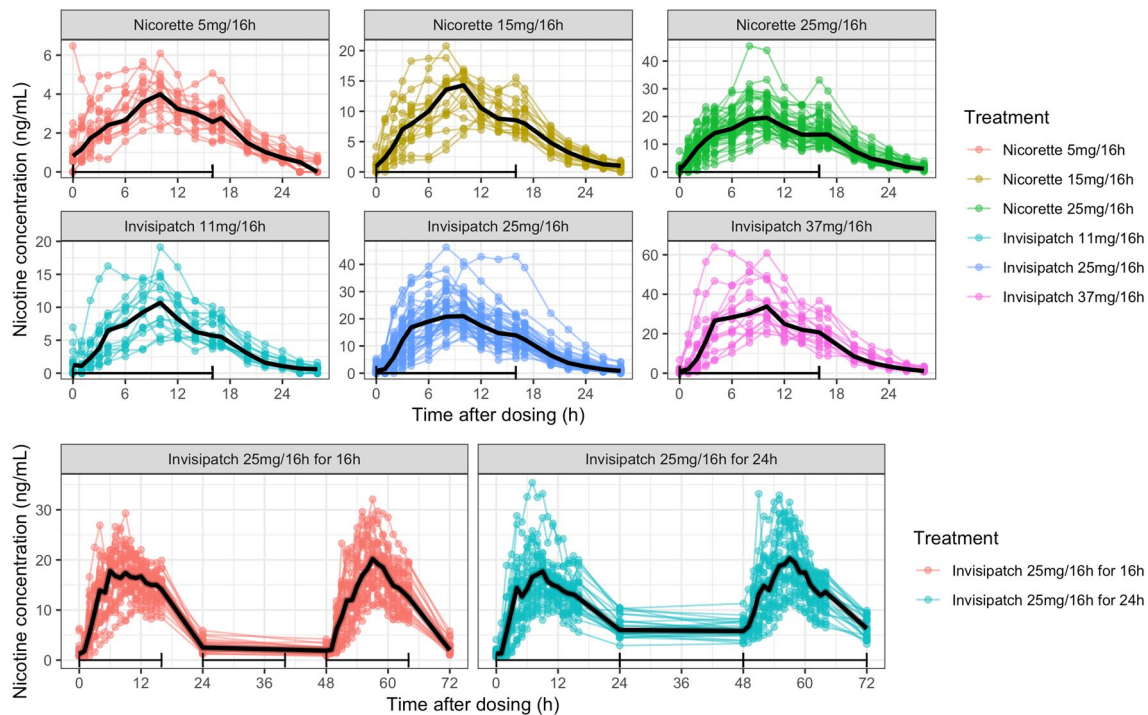
Fig. 9 Individual and median nicotine concentrations after single patch applications. Thin lines and dots are individual concentrations, thick black lines are median concentrations. Horizontal black lines indicate the patch application interval

simulations from the model, comparing the pharmacokinetics after administration of Nicorette patch and Invisipatch are shown in Fig. 12.

4 Discussion

Capitalising on extensive research with multiple Nicorette formulations, large datasets of rich PK data from many single- and repeated-dose studies were included in our analyses to build PPK models for nicotine administered as iv infusions, orally ingested microtablets, transdermal patches, and mouth spray, chewing gum, lozenge and inhaler formulations designed for oromucosal absorption. Because of the large sample sizes, estimates of fixed and random effects in the models were initially expected, and then confirmed, to be more robust and precise compared to single-subject/single-study analyses mostly employed thus far in researching the pharmacokinetics of nicotine.

To our knowledge, only limited PPK modelling has been performed to date for oral nicotine (one study) [21], for nasal spray, gum, combustion cigarettes, and tobacco heating systems (eight studies) [22] and for transdermal nicotine (one study) [27] using data after patch removal only [27]. There was a frequent occurrence of quantifiable, sometimes significant, pre-dose residual nicotine concentrations across all studies

and formulations, likely from prior smoking as subjects were regular smokers instructed, but not forced, to be abstinent only for a limited period (12–36 h) prior to dosing. Handling this by using a hypothetical nicotine dose at the start of washout, and scaling the exposure using a hypothetical F appeared to describe this reasonably well and allowed for profiles with high pre-dose exposure to still be included in the analysis. The estimated hypothetical dose of pre-dose nicotine will not be an unbiased estimate, as it assumes that the nicotine was delivered as a bolus at the start of washout. However, as it is only a nuisance parameter, this is of little consequence. However, some of the estimated hypothetical nicotine doses at the start of the washout period were very high (over 100 mg), which likely indicates non-compliance with the requirement not to smoke during washout in these subjects. For reference, the typical dose of nicotine delivered from cigarette smoking is in the order of 0.3–2 mg per cigarette [2, 38, 39].

For iv nicotine, owing to the richness of data and the enhanced sensitivity of a population mixed-effects analysis combining data from all subjects across multiple studies, the data were significantly better ($p < 0.001$) described with a three-compartment rather than a two-compartment model as done by others [9, 11, 19, 20]. Consequently, a typical terminal elimination half-life of nicotine of 4.5 h was estimated, somewhat longer than the 1.7–3.4 h estimated

Table 6 Parameters of the final transdermal model

Parameter	Estimate	RSE (%)[a]	90% CI[b]	Shr. (%)[d]
Fixed-effects parameters				
F (%)	75.8	4.41	70.3–81.3	–
CLch24 (%)	11.6	9.41	9.78–13.4	–
Fr1 Nicorette (%)	40.0	4.92	36.8–43.3	–
Fr1 Invisipatch (%)	71.9	2.49	68.9–74.8	–
Lag time1 (h)	0.53	3.2	0.503–0.558	–
Lag time2 (h)	4.06	4.08	3.79–4.33	–
K_{rel} (h^{-1})	0.146	11.5	0.118–0.173	–
Fr_{dur1} Nicorette (%)	44.5	7.06	39.3–49.6	–
Fr_{dur1} Invisipatch (%)	96.2	0.624	95.3–97.2	–
K_{trs} (h^{-1})	3.62	14.8	2.74–4.51	–
Pre-washout nicotine dose (mg)	3.82	17.1	2.74–4.89	–
Random-effects parameters				
IIV Fr1	0.238	33.4	0.107–0.37	9.79
IIV K_{rel} (CV%)[c]	49.5	27.6	35.6–61.2	10.5
IIV Fr_{dur1}	0.498	45.7	0.123–0.873	33.4
IIV KTR (CV%)[c]	114	30.8	71.4–159	7.84
IIV pre-washout nicotine dose (CV%)[c]	121	29.8	76.5–169	22.7
IOV F (CV%)[c]	12.9	14	11.3–14.3	21.5
IOV pre washout nicotine dose (CV%)[c]	91	16.4	74.4–107	28.2
Residual variability				
Proportional residual error	0.19	0.913	0.187–0.193	6.95
Additive residual error (ng/mL)	0.257	4.3	0.239–0.276	–

IIV Fr1 and Fr_{dur1} on logit scale

CI confidence interval, *CV* coefficient of variation, *F* bioavailability, *IIV* inter-individual variability, *IOV* inter-occasion variability, *IV* intravenous, *(R)SE* (relative) standard error, *Shr.* shrinkage

[a]RSE on variance scale for variability estimates

[b]Asymptotic confidence interval derived from NONMEM standard errors

[c]CV = 100 × sqrt(exp(variance) − 1)

[d]Epsilon shrinkage is the overall shrinkage for related elements of the residual error

half-life in previous studies [9, 12]. Our estimate is likely to be unbiased as we did not exclude the BQL observations from the analysis.

The typical systemic plasma CL of nicotine for a 70-kg individual was estimated at 1.1 L/min, which is approaching hepatic blood flow and in the 0.8–1.8 L/min range reported in previous studies [7–11]. The typical volume of distribution at steady state of nicotine was 4.2 L/kg, which is somewhat higher than the 1.8–3.3 L/kg range reported previously [7–12]. This is compatible with our ability to describe a slower phase in the systemic disposition of nicotine, which accounts for 61% of the area under the curve.

For oral nicotine, the *F* estimate was 40% in the repeated-dose study 92NNBT005 in 20 subjects. This estimate is in the middle of the range of previously published estimates, 17–69% [9, 10, 12, 40]. The *F* estimate of 22% from the oral single-dose study, 93NNBT007, was not used in developing the PPK models for buccal NRT formulations as it is based on only six subjects, the

absorption was delayed and *F* was at the lower end of the published estimates. While the explanation for this difference is unknown, it may well be due to the tablets, which were designed to be taken sublingually, in this study being ingested whole, while they were chewed before swallowing in the repeated-dose study.

For the repeated-dose studies with oral nicotine, but also for the buccal formulations, many individual profiles, and even some mean profiles (e.g. for orally administered nicotine), showed that accumulation stopped, or concentrations even decreased, for part of the day. This appeared to start within 1–2 h (oral) and 3–5 h (buccal) of the first dose and lasted up to after the last observations. This phenomenon was modelled as a function of time, either on CL (time-dependent increase; for mouth spray, lozenge and inhaler) or on *F* (time-dependent decrease; for chewing gum). As these changes mainly affect pre-dose trough concentrations in the repeated-dose data, an effect on *F* or on CL has similar impact on overall concentration–time
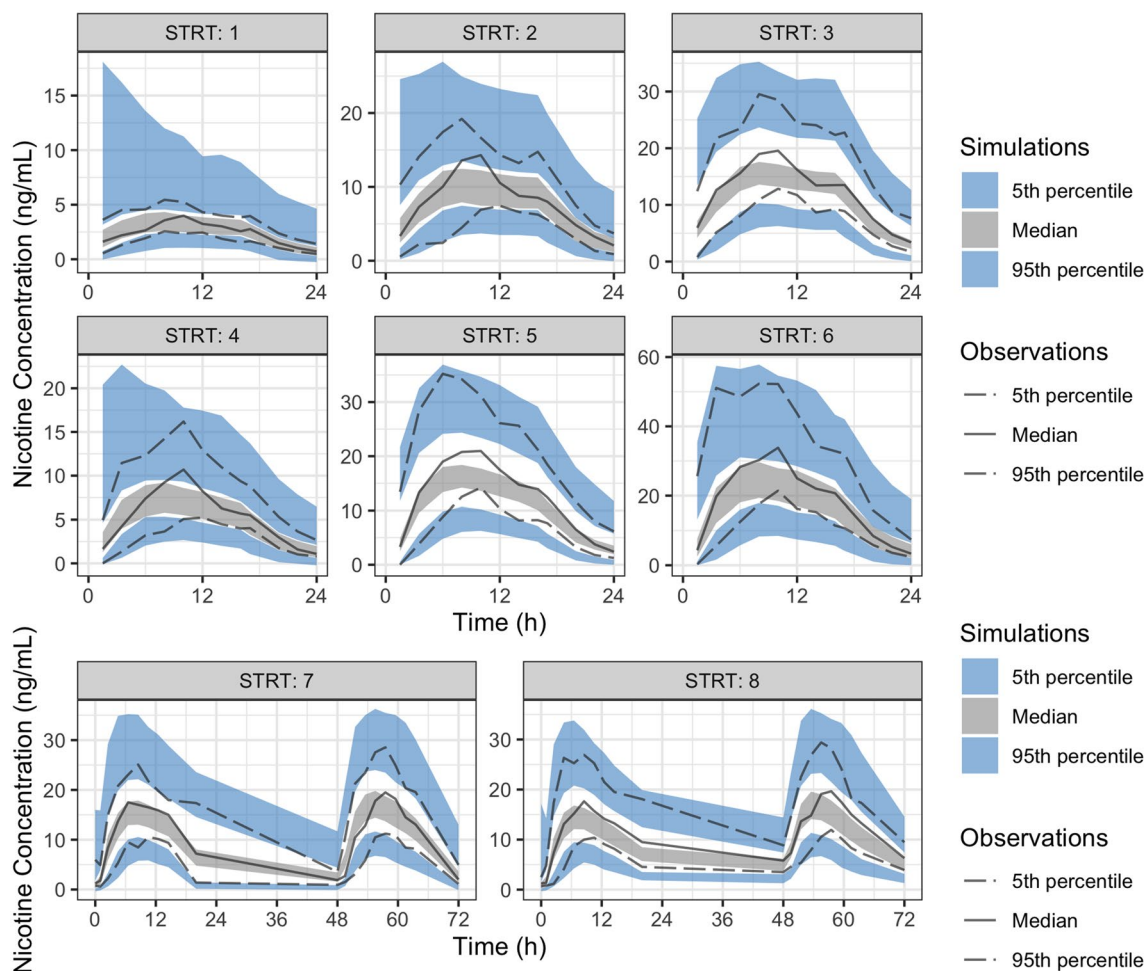
Fig. 10 Visual predictive check of final transdermal nicotine model after single and repeat dosing. Single doses: STRT 1: Nicorette 5-mg patch; STRT 2: Nicorette 15-mg patch; STRT 3: Nicorette 25-mg patch; STRT 4: Invisipatch 11-mg patch; STRT 5: Invisipatch 25-mg single and repeat dosing; STRT 6: Invisipatch 37-mg patch. Repeat dosing: STRT 7: Invisipatch 25-mg patch kept on for 16 h; STRT 8: Invisipatch 25 mg, patch kept on for 24 h. The solid line is the median, and the dashed lines are the 5th and 95th percentiles of observed concentrations. Areas indicate 95% confidence intervals based on the model, grey for median, blue for 5th and 95th percentiles

profiles. It is possible that the effect with the chewing gum data is also caused by a change in CL, but no such model was found that could describe the data well.

Diurnal variation in CL and an increased CL after meals have previously been observed by Gries et al. [11]. They found a diurnal variation in CL of ± 14% and a meal effect of +40%. This is in the same order of magnitude as what was observed in the current analysis. As nicotine is a high extraction ratio drug, CL can be expected to change with hepatic blood flow changes, such as can be caused by changes in physical activity, and by food intake.

For buccal nicotine, the absorption of nicotine from mouth spray, gum, lozenge and inhaler is rapid with peaks occurring shortly after the end of dosing. However, exploring individual profiles, absorption appears to be variable, with many subjects displaying a distinct double peak. The

second peak is likely due to intestinal absorption of swallowed nicotine.

The estimated fraction of swallowed nicotine was lowest for chewing gum (55%) followed by mouth spray (61%), inhaler (67%) and lozenge (69%). Estimation of the fraction swallowed is influenced by two assumptions made when modelling buccal formulations: fixing the oral F to 40% and assuming a F of the oromucosally absorbed fraction to be complete. The rank order and relative proportions of the fractions swallowed, however, do not depend on these assumptions. The differences in fraction swallowed between mouth spray, inhaler and lozenge remain small. This leads to a similar exposure after administration of chewing gum as after the other formulations, even though only part of the dose (on average 64–79%) is released from the chewing
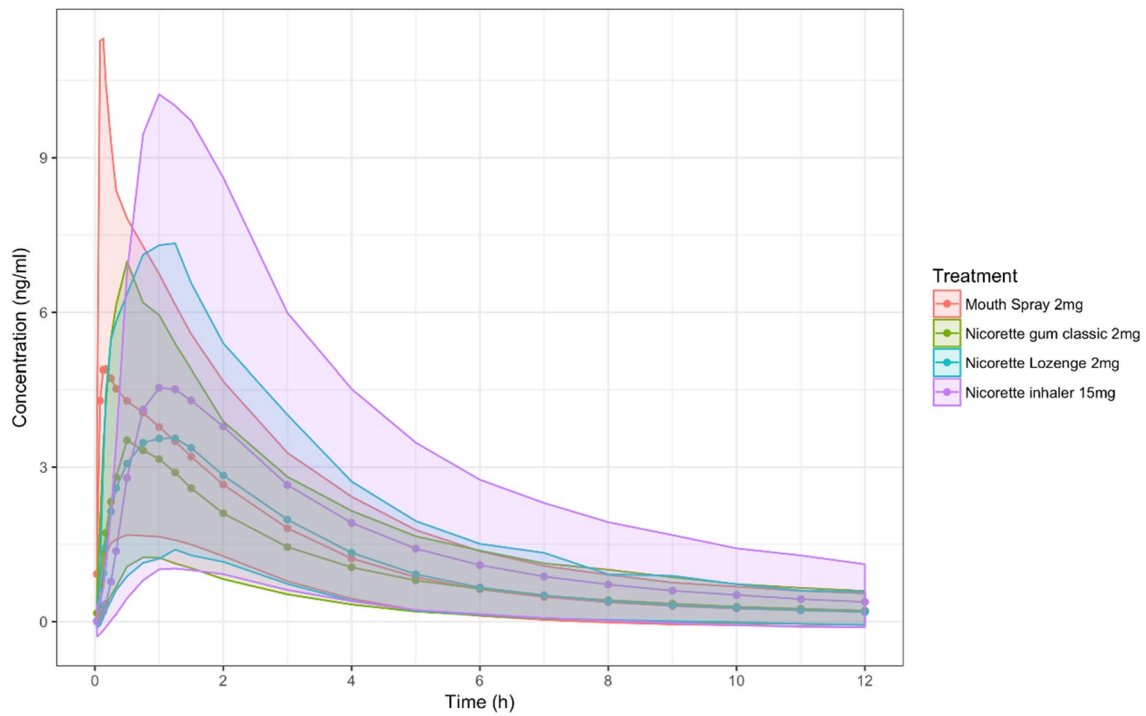
Fig. 11 Simulated single-dose profiles after administration of a 2-mg mouth spray, chewing gum, and lozenge, and a 15-mg inhaler. Lines are means; areas are 90% prediction intervals
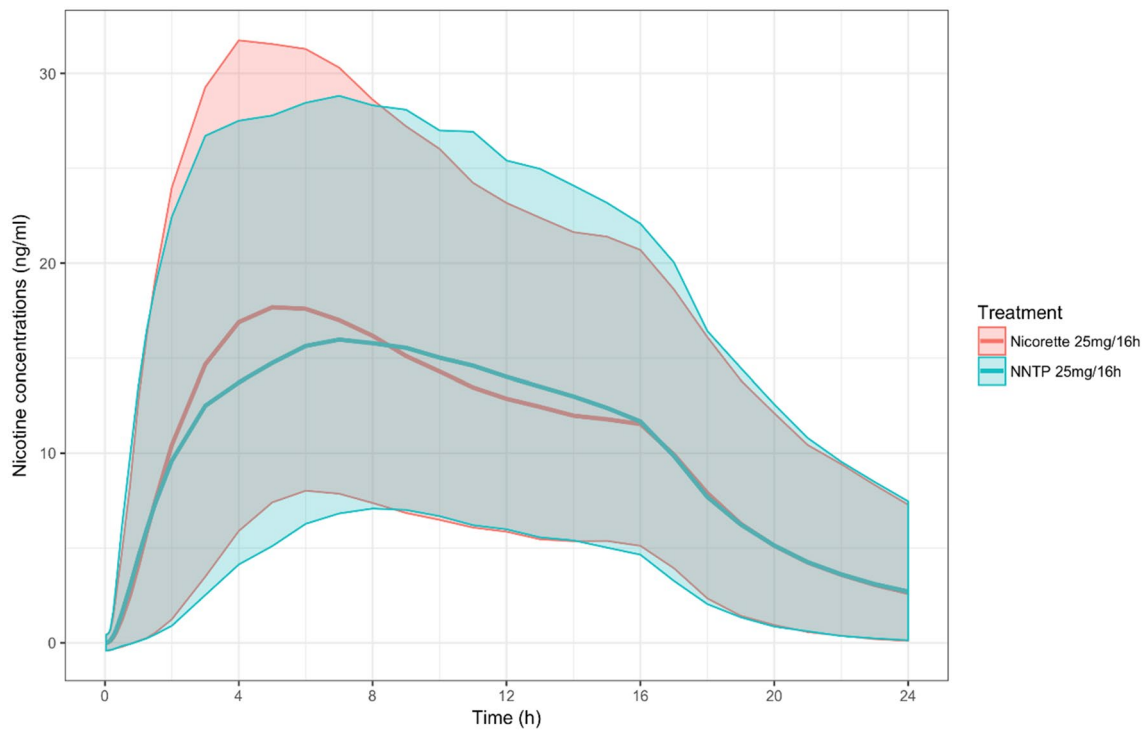

Fig. 12 Simulated single-dose profiles for Nicorette patch 25 mg/16 h and Invisipatch 25 mg/16 h (NNTP). Lines are means; areas are 90% prediction intervals

gum. When dose normalising for the average dose released, the predicted relative exposure is highest for chewing gum.

For several of the buccal formulations, the fraction of nicotine that is swallowed appeared to increase with dose. This leads to a lower overall F for higher doses, as the F of intestinally absorbed nicotine is lower than the oromucosally absorbed nicotine. One possible reason for this is the potentially irritating effects of nicotine in the oral cavity, which may lead to increasing saliva production at higher doses.

The K_a was fastest for Nicorette chewing gum, followed by mouth spray, lozenge, and Freshmint/Freshfruit-coated chewing gum, and, with a much slower K_a, for the inhaler. In Fig. 11, it can clearly be seen that nicotine concentrations increase most rapidly after the mouth spray, followed by chewing gum, lozenge and finally inhaler. This apparent discrepancy between K_a and the rate of increase in concentrations is owing to the absorption of nicotine from chewing gum being rate limited by the nicotine release from the formulation as the release rate constant, 2.8 h^{-1}, is much slower than the K_a of 9–26 h^{-1}.

For transdermal nicotine, the data were best described by a model with two parallel pathways for release of nicotine from the patch, zero-order release until patch removal and first-order release for an estimated fraction of the time of patch application, followed by absorption of nicotine though three serial transit compartments with a transit rate constant K_{tr} of 3.6 h^{-1}, corresponding to a mean residence time of 1.1 h. The release part of the model resembles that of the model of Gabrielsson and Weiner [41]. While using a different functional form, the transit compartment model used for the absorption part can be expected to give similar predictions as the Weibull model used by Linakis et al. [27].

The F of nicotine released from both patch types (i.e. Nicorette patch and Invisipatch) was estimated at 76%, which is in the range of 68–82% previously reported [9, 15]. To account for a lower than expected accumulation upon repeated dosing, CL was modelled to increase by 12% from 24 h after the first dose onwards. A plausible biological explanation for this is missing at this time. Additionally, for buccal formulations, an apparent increase in CL over time was observed, albeit earlier.

Two patch products were included in the dataset: Nicorette patch and Invisipatch. The estimated fraction of the dose released through the first-order process differed between products, 40% for Nicorette patch and 72% for Invisipatch, and the estimated model parameters for nicotine release (Fr1, lag time, Frdur1) were fairly different. These differences could be related to design differences of the two patch formulations: for the Nicorette patch, the adhesive layer in contact with skin contains only a small amount of nicotine at product release whereas for Invisipatch the layer in contact with the skin already has a maximum nicotine concentration. However, comparing the simulated profiles

of the two patches (Fig. 12), nicotine concentrations overlap to a large extent and no meaningful differences in efficacy or safety should be expected. Previously, the two patch formulations were demonstrated to be bioequivalent [42].

The PPK models developed in this research were used to conduct nicotine exposure–response analyses linking nicotine exposure to momentary craving and smoking cessation, as published elsewhere [28, 43]. The PPK and the exposure–response models were used to build a simulation platform that is being used to (i) maximise the value of the existing products by understanding the effect of different dosing scenarios, including combinations treatments, in momentary craving and (ii) streamline the development of new NRT products by leveraging the nicotine PKPD knowledge in identifying the appropriate nicotine dose and delivery rate of a new product to achieve a desired momentary craving effect, and optimising the PKPD information that needs to be collected from the clinical studies of new products or combinations.

Despite the wealth of available data, there were data-related limitations to our analyses. The studies included in the analyses were not designed to be included in any integrated modelling or other meta-analyses. These studies were conducted over a 19-year period. The designs of the studies, however, were remarkably similar and for each formulation the studies were carried out at the same clinical unit and bioanalytical laboratory. The populations included were homogeneous as to demographic and other subject characteristics, in particular regarding age and body size characteristics. Furthermore, there were very few non-Caucasian individuals in the dataset. Therefore, the results may not be representative for all smoking populations globally.

Finally, we tried to simultaneously model iv and extravascular data, without success in terms of numerical convergence and stability of the model runs. This may be due to the use of the LAPLACIAN method in NONMEM, which can be unstable, but which was necessary for fitting the iv data, owing to the large number of observations BQL. Therefore, separate models were developed for oral, buccal and transdermal nicotine for which the CL and disposition parameters, including their IIVs, were fixed to the estimates of the final iv model. This is considered a reasonable approach as the parameters of the iv model are based on a large sample. When doing this, fits of the extravascular data generally appeared to be unbiased, and F estimates were reasonable.

5 Conclusions

We developed PPK for iv, oral, buccal and transdermal nicotine using large rich datasets. Key PK parameters of nicotine were reliably estimated, with typical values for CL of 67 L/h,

volume of distribution of 4.3 L/kg and terminal half-life of 4.5 h. Typical values for oral and transdermal *F* were 40% and 76%, respectively.

For mouth spray, gum, lozenge and inhaler, all designed for oromucosal absorption of nicotine, an estimated 55–69% of the dose was swallowed and subsequently available for intestinal absorption. A time-dependent increase in CL or decrease in *F* was required to model the lower than expected plasma concentrations at steady state for repeated-dose oral and buccal administrations. These models can be, and have been, used for Bayesian prediction of concentration–time profiles for use in exposure–response analysis [28], and for simulation of various dosing scenarios.

Declarations

Conflict of interest Per O. Olsson Gisleskog performed the research while employed by SGS Exprimo NV, but has no conflicts of interest that are directly relevant to the content of this article. Juan José Perez Ruixo, Åke Westin, Anna C. Hansson and Paul A. Soons are (former) employees of affiliated companies of Johnson & Johnson.

Ethics approval All clinical trials included in this research were approved by the Institutional Review Boards of the Universities of Lund (26 studies), Linköping (2 studies) or Gothenburg (1 study), Sweden.

Consent to participate Informed consent was obtained from each subject, in all studies included in this research.

Consent for publication Not applicable.

Availability of data and material Not applicable.

Code availability Model codes are included in Electronic Supplemental Materials.

Author contributions All authors contributed to the research conception and design. Data collection was performed by AW and POG. Data analysis and research were performed by POG. The first draft of the manuscript was written by POG and PS. All authors commented on previous versions of the manuscript and read and approved the final manuscript.

References

1. World Health Organization. WHO global report: mortality attributable to tobacco. 2012. https://apps.who.int/iris/bitstream/10665/44815/1/9789241564434_eng.pdf. Accessed 13 Dec 2017.
2. World Health Organization. WHO report on the global tobacco epidemic: monitoring tobacco use and prevention policies. https://apps.who.int/iris/bitstream/10665/255874/1/9789241512824-eng.pdf. Accessed 3 Aug 2018.
3. GBD 2017 Risk Factors Collaborators. Global, regional, and national comparative risk assessment of 84 behavioural, environmental and occupational, and metabolic risks or clusters of risks for 195 countries and territories, 1990–2017: a systematic analysis for the Global Burden of Disease Study 2017. Lancet. 2018;392:1923–94.
4. Benowitz NL & Society for Research on Nicotine and Tobacco. Nicotine safety and toxicity. Oxford: Oxford University Press; 1998.
5. Hartmann-Boyce J, Chepkin SC, Ye W, Bullen C, Lancaster T. Nicotine replacement therapy versus control for smoking cessation. Cochrane Database Syst Rev. 2018;5:CD000146. https://doi.org/10.1002/14651858.CD000146.pub5.
6. Shields PG, Herbst RS, Arenberg D, Benowitz NL, Bierut L, Bylund Luckart J, et al. Smoking cessation, Version 1.2016, clinical practice guidelines in oncology. J Natl Compr Cancer Netw. 2016;14:1430–68.
7. Hukkanen J, Jacob P, Benowitz NL. Metabolism and disposition kinetics of nicotine. Pharmacol Rev. 2005;57:79–115.
8. Benowitz NL, Hukkanen J, Jacob P. Nicotine chemistry, metabolism, kinetics and biomarkers. In: Henningfield JE, London ED, Pogun S, editors. Nicotine psychopharmacology. Handbook of experimental pharmacology, vol. 192. Berlin: Springer; 2009. p. 29–60.
9. Benowitz NL, Jacob P, Denaro C, Jenkins R. Stable isotope studies of nicotine kinetics and bioavailability. Clin Pharmacol Ther. 1991;49:270–7.
10. Zins BJ, Sandborn WJ, Mays DC, Lawson GM, McKinney JA, Tremaine WJ, et al. Pharmacokinetics of nicotine tartrate after single-dose liquid enema, oral, and intravenous administration. J Clin Pharmacol. 1997;37:426–36.
11. Gries JM, Benowitz N, Verotta D. Chronopharmacokinetics of nicotine. Clin Pharmacol Ther. 1996;60:385–95.
12. Compton RF, Sandborn WJ, Lawson GM, Sheets AJ, Mays DC, Zins BJ, et al. A dose-ranging pharmacokinetic study of nicotine tartrate following single-dose delayed-release oral and intravenous administration. Aliment Pharmacol Ther. 1997;11:865–74.
13. Hughes JR. Dependence on and abuse of nicotine replacement medications: an update. In: Benowitz NL, editor. Nicotine safety and toxicology. Oxford: Oxford University Press; 1998. p. 47–157.
14. Benowitz NL, Chan K, Denaro CP, Jacob P. Stable isotope method for studying transdermal drug absorption: the nicotine patch. Clin Pharmacol Ther. 1991;50:286–93.
15. Gupta SK, Benowitz NL, Jacob P, Rolf CN, Gorsline J. Bioavailability and absorption kinetics of nicotine following application of a transdermal system. Br J Clin Pharmacol. 1993;36:221–7.

16. Fant RV, Henningfield JE, Shiffman S, Strahs KR, Reitberg DP. A pharmacokinetic crossover study to compare the absorption characteristics of three transdermal nicotine patches. Pharmacol Biochem Behav. 2000;67:479–82.

17. Benowitz NL. Clinical pharmacology of transdermal nicotine. Eur J Pharm Biopharm. 1995;41:168–74.

18. Johansson CJ, Olsson P, Gunnarsson PO, Säwe U. Pharmacokinetics of a 16-hour transdermal nicotine patch. Clin Drug Investig. 1996;12:198–206.

19. Molander L, Hansson A, Lunell E, Alainentalo L, Hoffmann M, Larsson R. Pharmacokinetics of nicotine in kidney failure. Clin Pharmacol Ther. 2000;68:250–60.

20. Molander L, Hansson A, Lunell E. Pharmacokinetics of nicotine in healthy elderly people. Clin Pharmacol Ther. 2001;69:57–65.

21. Levi M, Dempsey DA, Benowitz NL, Sheiner LB. Population pharmacokinetics of nicotine and its metabolites. I. Model development. J Pharmacokinet Pharmacodyn. 2007;34:5–21.

22. Marchand M, Brossard P, Merdjan H, Lama N, Weitkunat R, Lüdicke F. Nicotine population pharmacokinetics in healthy adult smokers: a retrospective analysis. Eur J Drug Metab Pharmacokinet. 2017;42:943–54.

23. Molander L, Lunell E. Pharmacokinetic investigation of a nicotine sublingual tablet. Eur J Clin Pharmacol. 2001;56:813–9.

24. Molander L, Lunell E, Andersson A-B, Kuylenstierna F. Dose released and absolute bioavailability of nicotine from a nicotine vapor inhaler. Clin Pharmacol Ther. 1996;59:394–400.

25. Hansson A, Rasmussen T, Kraiczi H. Single-dose and multiple-dose pharmacokinetics of nicotine 6 mg gum. Nicotine Tob Res. 2017;19:477–83.

26. Kraiczi H, Hansson A, Perfekt R. Single-dose pharmacokinetics of nicotine with a novel mouth spray form of nicotine replacement therapy. Nicotine Tob Res. 2011;13:1176–82.

27. Linakis MW, Rower JE, Roberts JK, Miller EI, Wilkins DG, Sherwin CMT. Population pharmacokinetic model of transdermal nicotine delivered from a matrix-type patch. Br J Clin Pharmacol. 2017;83:2709–17.

28. Germovsek E, Hansson A, Kjellsson MC, Perez Ruixo JJ, Westin Å, Soons PA, et al. Relating nicotine plasma concentration to momentary craving across four nicotine replacement therapy formulations. Clin Pharmacol Ther. 2020;107(1):238–45. https://doi.org/10.1002/cpt.1595.

29. Beal SL, Sheiner LB, Boeckmann AJ, Bauer RJ. NONMEM users guides. Ellicott City: Icon Development Solutions; 1989–2015.

30. Lindbom L, Pihlgren P, Jonsson N. PsN-Toolkit: a collection of computer intensive statistical methods for non-linear mixed effect modeling using NONMEM. Comput Methods Progr Biomed. 2005;79:241–57.

31. R Development Core Team. R: A language and environment for statistical computing. Vienna: R Foundation for Statistical Computing; 2017.

32. US Food and Drug Administration. Guidance for industry: population pharmacokinetics. February 1999. https://www.fda.gov/downloads/Drugs/GuidanceComplianceRegulatoryInformation/Guidances/ucm072137.pdf. Accessed 13 Dec 2017.

33. Committee for Medicinal Products for Human use (CHMP). Guideline on reporting the results of population pharmacokinetic analyses. CHMP/EWP/185990/2006. Adopted by CHMP 21 June 2007. https://www.ema.europa.eu/docs/en_GB/document_library/Scientific_guideline/2009/09/WC500003067.pdf. Accessed 13 Dec 2017.

34. SGS Exprimo. https://www.exprimo.com/simulo. Accessed 29 May 2019.

35. Bergstrand M, Karlsson MO. Handling data below the limit of quantification in mixed effect models. AAPS J. 2009;11:371–80.

36. Boxenbaum H. Interspecies variation in liver weight, hepatic blood flow, and antipyrine intrinsic clearance: extrapolation of data to benzodiazepines and phenytoin. J Pharmacokinet Biopharm. 1980;8(2):165–76.

37. Karlsson MO, Holford N. A tutorial on visual predictive checks. 2008. www.page-meeting.org/?abstract=1434. Accessed 17 Jan 2018.

38. Benowitz NL, Jacob P. Daily intake of nicotine during cigarette smoking. Clin Pharmacol Ther. 1984;35:499–504.

39. Schroeder MJ, Hoffman AC. Electronic cigarettes and nicotine clinical pharmacology. Tob Control. 2014;23(Suppl 2):ii30–5.

40. Sellers EM, Kaplan HL, Tyndale RF. Inhibition of cytochrome P450 2A6 increases nicotine's oral bioavailability and decreases smoking. Clin Pharmacol Ther. 2000;68:35–43.

41. Gabrielsson J, Weiner D. Pharmacokinetic and pharmacodynamic data analysis: concepts and applications. 2nd ed. Stockholm: Swedish Pharmaceutical Press; 1997. p. 551–5.

42. Medicines and Healthcare products Regulatory Agency. UK public assessment report on NICORETTE Invisi Patch, PL 155 13/0159-0161, May 2016. https://www.mhra.gov.uk/home/groups/par/documents/websiteresources/con036311.pdf. Accessed 17 Jan 2018.

43. Germovsek E, Hansson A, Karlsson MO, Westin Å, Soons PA, Vermeulen A, et al. A time-to-event model relating integrated craving to risk of smoking relapse across different nicotine replacement therapy formulations. Clin Pharmacol Ther. 2020. https://doi.org/10.1002/cpt.2000 (**Epub ahead of print**).

Affiliations

Per O. Olsson Gisleskog[1,6] · **Juan José Perez Ruixo**[2] · **Åke Westin**[3] · **Anna C. Hansson**[4] · **Paul A. Soons**[5]

1 SGS Exprimo NV, Life Science Services, London, UK

2 Janssen Research & Development, Quantitative Sciences, Beerse, Belgium

3 McNeil AB, Global Medical Affairs and Clinical Research, Helsingborg, Sweden

4 McNeil AB, Clinical Science, Helsingborg, Sweden

5 Janssen Pharmaceutica NV, Alliance Management, Turnhoutseweg 30, 2340 Beerse, Belgium

6 Present Address: POG Pharmacometrics, London, UK